Langmuir

Article

pubs.acs.org/Langmuir

Dynamic Wetting of Hydrophobic Polymers by Aqueous Surfactant and Superspreader Solutions

Xiang Wang,[†] Longquan Chen,[†] Elmar Bonaccurso,*[,†] and Joachim Venzmer[‡]

[†]Center of Smart Interfaces, Technical University Darmstadt, 64287 Darmstadt, Germany

[‡]Evonik Industries AG, Goldschmidtstrasse 100, 45127 Essen, Germany

Supporting Information

ABSTRACT: In this paper, we comparatively investigated the wetting performance of aqueous surfactant solutions in a wide range of concentrations, including conventional ionic surfactants (CTAB, SDS) and two nonionic polyether-modified trisiloxane surfactants (TSS6/3, TSS10/2), over hydrophobic polypropylene substrates. In all cases, scaling analysis of the experimental data of spreading drops showed that the early spreading stage was dominated by inertia and that the duration of this stage was not influenced by the addition of surfactant. For conventional surfactant solutions, we only observed the inertia-dominated spreading stage before the drops stopped wetting with a finite stable contact angle. For both trisiloxane surfactants, after the inertial stage we observed a second viscosity-dominated spreading stage. In this stage, TSS10/2 showed an enhanced wetting capability independent of its concentration, while TSS6/3 started to show a concentration-dependent spreading behavior that was fully developed in a third superspreading stage. Our findings suggest that the superspreading property of TSS6/3 began to take effect after a characteristic time, before which the superspreading TSS6/3 and the nonsuperspreading TSS10/2 behaved similarly. Power law fits to the superspreading regime are in agreement with an interpretation of Marangoni flows resulting from surface tension gradients.

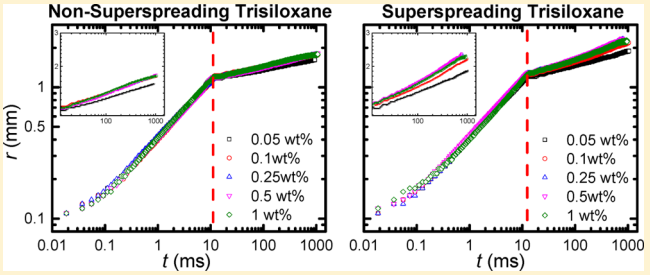

1. INTRODUCTION

The enhancement of the wetting ability of aqueous solutions over hydrophobic substrates is significant in diverse agricultural and industrial applications, such as herbicide spreading, cosmetics, coating, printing, and many others.[1−4] Surfactants are widely used as additives to facilitate spreading of water drops on solid substrates by reducing the surface tension of the liquids. Discovered in the 1960s,[5,6] certain low molecular weight siloxane surfactants greatly improve the wetting ability of dilute aqueous solutions over hydrophobic substrates, which are not so easily wetted by pure water or aqueous solutions of conventional ionic surfactants (e.g., the cationic cetyltrimethyl ammonium bromide, CTAB, or the anionic sodium dodecyl sulfate, SDS). In recent years, trisiloxane surfactants attracted considerable attention in both scientific and industrial fields. The surface tension of aqueous trisiloxane surfactant solutions even at a low concentration (∼0.1 wt %) is significantly lower (∼22 mN/m) than that of pure water (∼72 mN/m) and the wetting ability of such solutions is dramatically improved.[1] Within tens of seconds, aqueous trisiloxane solutions can spread over hydrophobic substrates into a thin film with a final macroscopic contact angle of zero, and the overall wetting area is as much as 50 times larger than that of water and 25 times larger than that of conventional aqueous surfactant solutions.[7] As a result, certain trisiloxane surfactants are called "superspreaders" and the wetting process of aqueous superspreader solutions is referred to as "superspreading".[2,8−11]

Pioneered by Ananthapadmanabhan and co-workers,[1] numerous theoretical and experimental investigations have been performed to understand the mechanism underlying the superspreading behavior of aqueous trisiloxane solutions on hydrophobic substrates. Commercially available trisiloxane surfactant, Silwet L-77 (Momentive), has been widely investigated in numerous papers.[8,12−14] The experiments mainly involved measuring dynamic contact angles and monitoring the shape of drops spreading on solid substrates with varying hydrophobicity. One of the commonly used methods to analyze spreading is matching the curves of the spreading radius r versus the spreading time t with a power law, $r \propto t^{\alpha}$, with α being the so-called wetting exponent.[14−18] However, different exponents α were reported even for similar aqueous superspreader solutions.[14,16,19] The incompatible results may stem from several reasons. For example, most commercial surfactants are not single species but mixtures of different homologues. Moreover, aqueous trisiloxane surfactant solutions are not stable and slowly hydrolyze over time, depending on pH, concentration, and temperature.[20] Also different hydrophobic substrates such as polystyrene, Parafilm, or polypropylene have been used in the experiments, which makes it difficult to compare results. Lee et al.[18] investigated the

Received: October 15, 2013
Revised: November 2, 2013
Published: November 4, 2013

spreading dynamics of trisiloxanes solutions of increasing solubility on thin aqueous layers and found that the spreading process could be separated into a first fast stage ($10 \lesssim t \lesssim 100$ ms) and a second slower stage ($t \gtrsim 100$ ms). Increasing the solubility of trisiloxanes resulted in higher wetting velocities. It should be noted that superspreader solutions also fail to superspread on substrates too hydrophobic, such as PTFE. The potential influences of surface energy and surface roughness of the solid substrates cannot be neglected. Therefore, surfactants, substrates, and experimental conditions should be selected properly to make sure the superspreading phenomenon occurs and can be analyzed.

A number of hypotheses have been put forward to explain the superspreading ability of trisiloxane surfactants, such as the unique molecular structure, the aggregation of surfactant molecules to form micelles, vesicles, or lamellae, the adsorbability of surfactant molecules to the solid−liquid interface, and so on. Ananthapadmanabhan et al.[1] proposed that superspreading was due to the unique hammer-like geometry of trisiloxane surfactants, which lead to a favorable molecular orientation at the leading edge of spreading drops. Hill et al.[11] investigated the spreading properties of various superspreaders including analogous linear trisiloxane surfactants and showed that the unusual shape of the surfactant molecule was not an explanation of the enhanced wetting properties. Instead, they proposed that end-capping groups of surfactants had a significantly greater impact on the phase behavior than the structure of the siloxane hydrophobe. Specific surfactant aggregates in solution, such as vesicles, were stated to be an important factor for superspreading in several studies.[1,2,8,9] The authors suggested that the rapid spreading occurred only when surfactant-rich phases were present, but this was questioned in ref 14. A possible link between the formation of bilayer-like aggregates of surfactants and superspreading was postulated by many authors.[2,9,10,21,22] The reason lies in the possibility that the bilayer microstructure enables an efficient and rapid transfer of surfactant molecules to the liquid−vapor and liquid−substrate interfaces. It was pointed out that the ability to form bilayer-like aggregates, such as vesicles and lamellar phases, is common to all superspreading trisiloxane surfactants, while trisiloxane surfactants carrying longer hydrophilic groups only form micelles and do not superspread.[9] The effect of Marangoni flows induced by surface tension gradients arising during spreading was suspected to be a major driving force for the superspreading process.[8,12,14,16,23] Gradients in surface tension create a dragging force resulting in fluid motion in the adjacent bulk liquid in the direction of increasing surface tension. However, the direction of the surface tension gradient remains an open question. Zhu et al.[8] suggested that the Marangoni flow was located in the precursor film ahead of the drop rim that was formed in saturated or supersaturated water vapor phase. Suggestions that superspreading was driven by the Marangoni flow located along the stretching drop surface or directed along the height of the drop were reported in refs 14 and 16.

When a drop is deposited on a solid substrate, the out-of-balance interfacial force $\gamma_{lv}(\cos\theta - \cos\theta_0)$ drives the liquid to move in the direction of restoring equilibrium, while the inertia of the drop, the friction at the contact line, and the viscous dissipation within the drop resist the spreading of the liquid. γ_{lv} is liquid−vapor surface tension; θ and θ_0 are dynamic and static contact angles, respectively. The wetting of solid substrates by pure liquids with constant surface tension has been investigated for more than two centuries.[24,25] However, it was only in recent years that the first several milliseconds of the spreading process were experimentally accessible by the advent of high speed cameras. For both, complete and partial wetting systems, an inertial wetting regime was found prior to the viscous wetting regime in experimental and theoretical studies.[26−28] During the inertial regime ($t \lesssim 10$ ms), the base contact radius increases as $r \propto t^{\alpha}$ with $\alpha = 1/2$ for $t \lesssim 0.1$ ms or for fully wettable substrates and $1/5 \lesssim \alpha \lesssim 1/2$ for $t \gtrsim 0.1$ ms for partially wettable substrates. However, there is a lack of experimental data about the early wetting dynamics of aqueous surfactant solutions, which could help clarifying whether surfactants play a role in the early spreading stages, or only later. In the above-mentioned literature about surfactant-enhanced spreading, most studies were carried out at spreading time scales from seconds to minutes.

In this work, we carried out a comparative study of the wetting dynamics of aqueous conventional ionic surfactants and trisiloxane solutions with different concentrations on a hydrophobic substrate, a polypropylene film. High speed video microscopy with time resolution of 0.019 ms, or 54,000 fps, was employed to record the fast wetting dynamics of aqueous surfactant solutions. We identified that with surfactants, inertia was still the major opposing force for drop spreading during the early stage. Nevertheless, surfactant-enhanced spreading was different for conventional ionic surfactants and trisiloxane solutions. For ionic surfactant solutions, before equilibrium was reached only one spreading stage was observed. In contrast, two spreading stages were found for both aqueous trisiloxane solutions, and the superspreading phenomenon was observed only for TSS6/3 in a late stage ($t \gtrsim 100$ ms). However, the superspreading dynamics took a certain time to develop and before this time superspreader and nonsuperspreader behaved similarly.

2. DYNAMIC WETTING MODELS

2.1. Fast Wetting Dynamics. In the early stages of dynamic wetting, spreading is dominated by inertia rather than viscosity, which was verified in many papers.[26−29] Bird and co-workers[28] proposed a scaling analysis by considering the energy balance during spreading. They experimentally found and theoretically proposed that the spreading radius grows with time according to

$$r \propto t^{\alpha} \tag{1}$$

The wetting exponent α is only dependent on the substrate wettability, with $\alpha \propto (F(\theta_0) + \cos\theta_0)^{1/2}$, where $F(\theta_0)$ is some undetermined function.

With a slight modification of existing works,[26,28] but based on slightly different assumptions, Chen et al.[29] derived the same scaling law with $1/5 \lesssim \alpha \lesssim 1/2$. The inertial stage normally lasts for a characteristic inertial time $\tau_c \propto (\rho R^3/\gamma)^{1/2}$.[28] R is the initial drop radius and ρ is the liquid density. However, it was found that the actual inertial time τ is always larger than τ_c.[26−28] One possible explanation is that the inertial wetting lasts as long as the capillary wave generated upon contact of drop and surface propagates along the drop.[28] Following the vibration model of suspended drops proposed by Lamb,[30] a linear relationship between τ and τ_c, $\tau \approx 2.2\tau_c$, was obtained.[27] The authors experimentally proved that the actual duration of the inertial spreading was slightly longer, because the constantly growing contact radius of the drop would slow the propagation of the capillary wave.

dx.doi.org/10.1021/la403994y | Langmuir 2013, 29, 14855−14864

2.2. Slow Wetting Dynamics. On partially and completely wetting substrates, a slower viscous wetting stage, following the inertial stage, was observed.[31−33] The unbalanced horizontal capillary driving force is counteracted by viscous dissipation in the bulk liquid or by friction of the moving rim of the drop (the so-called three-phase contact line or TPCL). The two principal approaches to describe the dominating channels of energy dissipation are the hydrodynamic and the molecular kinetic theory models.[34−37]

Hydrodynamic Model (HD). The HD model, typically using the lubrication approximation, considers that the capillarity-driven spreading is opposed by viscous dissipation in the liquid.[24,36,37] To prevent the divergence of viscous dissipation at the drop rim, it is assumed that the liquid slips in a region near the wetting line. This leads to the dependence of the dynamic contact angle on the contact line velocity$V$:[36]

$$g(\theta) = g(\theta_0) + \frac{\eta V}{\gamma_{lv}} \ln\left(\frac{L}{L_s}\right) \tag{2}$$

where g is a rather complicated integrand and η is the liquid viscosity. L characterizes a macroscopic length scale (in the order of the drop size), and L_s denotes a microscopic slip length, which is in the order of a molecular size.[38] The free parameters in eq 2 are the static contact angle θ_0 and $\ln(L/L_s)$, which is expected to be ∼10.

For contact angles smaller than 135°, $g(\theta) \approx \theta^3/9$. Equation 2 can then be simplified to[37]

$$\theta^3 = \theta_0^3 + 9\frac{\eta V}{\gamma_{lv}} \ln\left(\frac{L}{L_s}\right) \tag{3}$$

For complete wetting, that is, $\theta_0 \sim 0°$, one can find the relationship between spreading radius r and spreading time t

$$r(t) \propto t^{1/10} \tag{4}$$

which has been verified experimentally[39−41] and is mostly referred to as Tanner's law.[32]

The Molecular-Kinetic Theory (MKT). Blake[34] was the first to account for a microscopic dissipation process happening in the close vicinity of the TPCL. In the MKT model, contact-line motion is mainly described in terms of individual molecular jumps, with an equilibrium frequency K_0 (typically $\sim 10^6$ s^{-1}) and a displacement distance λ (typically ∼1 nm). The relationship between dynamic contact angle and velocity is given by

$$V = 2K_0\lambda \sinh\left[\frac{\gamma_{lv}\lambda^2}{2kT}(\cos\theta_0 - \cos\theta)\right] \tag{5}$$

where k is the Boltzmann constant and T is the absolute temperature. If the argument of sinh is small, eq 5 simplifies to

$$V = \frac{K_0\lambda^3}{kT}\gamma_{lv}(\cos\theta_0 - \cos\theta) \tag{6}$$

Again, if $\theta_0 \sim 0°$ and θ is relatively small, eq 6 gives the time dependence of the base radius r with

$$r(t) \propto t^{1/7} \tag{7}$$

The above equation has also been validated experimentally and theoretically.[41,42]

2.3. Superspreading Dynamics. Nikolov et al.[13,14] proposed that the fast spreading of aqueous trisiloxane surfactants is driven by the surface tension gradient (Marangoni stress) that develops at the expanding liquid−vapor interface. They built a simple model based on the lubrication approximation to predict the spreading radius as a function of time under the action of a surface tension gradient.[14] The average spreading velocity V_{av} was simplified to

$$V_{av} \approx \frac{h(t)}{2\eta}\nabla\gamma(t) \tag{8}$$

$h(t)$ is the height of spreading drop, and $\nabla\gamma(t)$ is the surface tension gradient. In addition, the relation, $h(t) \propto 1/r^2(t)$, can be derived from mass conservation. The driving force of spreading is assumed to be a radial surface tension gradient over the drop surface, which is approximated as

$$\nabla\gamma(t) \approx \frac{\Delta\gamma(t)}{r(t)} \tag{9}$$

where $\Delta\gamma(t)$ is the difference between the surface tension near the contact line and the drop apex.

If $\Delta\gamma(t)$ was supposed to increase linearly with time, from eqs 8 and 9 the authors predicted the spreading radius versus time as $r \propto t^{1/2}$. Assuming $\Delta\gamma(t)$ was constant, they obtained $r \propto t^{1/4}$. This result was also reported by Rafai et al.[16] using similar arguments. However, it is unknown over what distance the Marangoni effect is active. As reported in ref 16, different options lead to a power law with different wetting exponents. If the surface tension gradient is established over a certain length of the precursor film ahead of the drop rim, the time dependence of spreading radius follows $r \propto t^{1/3}$. Moreover, one may expect that the surface tension gradient acts over the drop height, $\nabla\gamma(t) \approx (\nabla\gamma)/h$. In this case, simple dimensional analysis of eq 8 finds the drop radius increases linearly with time, $r \propto t$.

3. EXPERIMENTAL SECTION

3.1. Substrate and Surfactants. The hydrophobic polypropylene (PP) films (FORCO OPPB AT-OPAL) were purchased from 4P Folie Forchheim/Germany. Pure water exhibits a static contact angle of ∼97°, an advancing contact angle of ∼114°, and a receding contact angle of ∼88° on PP. Advancing and receding contact angles were measured by the sessile drop technique with a Profile Analysis Tensiometer (PAT1, SINTERFACE Technologies, Berlin, Germany) by inflating or deflating the drops. Note that we define our "static" contact angle as the angle when the contact line of the drop that spreads with a constant volume stops moving.

Cationic cetyltrimethyl ammonium bromide (CTAB) surfactant and anionic sodium dodecyl sulfate (SDS) surfactant were obtained from Sigma-Aldrich and Acros Organics, respectively. Nonionic trisiloxane surfactants TSS10/2 and TSS6/3 (denoted as M (D'E_nP_mOH) M, with n = 10, 6 and m = 2, 3 on average, respectively) were synthesized at Evonik Industries AG, Germany. These surfactants were used without further purification. Here, M represents the trimethylsiloxy group $(CH_3)_3SiO_{1/2}$−, the term D' stands for the $-O_{1/2}Si(CH_3)(R)O_{1/2}$−, where R is obtained from a mixture of ethylene oxide and propylene oxide (R = $-(CH_2)_3-O-(CH_2-CH_2-O-)_n-(CH_2-CH(CH_3)-O-)_m$).

Aqueous CTAB and SDS surfactant solutions were prepared using ultra pure water (18.2 MΩcm, Sartorius Arium 611, Göttingen, Germany). The concentrations studied were 0.1−3 times the critical micelle concentration (CMC), where CMC refers to the critical concentration above which micelle aggregation forms in aqueous surfactant solutions. The CMC values are 9.6×10^{-4} and 8.3×10^{-3} mol/L for CTAB and SDS, respectively.[43] Aqueous TSS10/2 and TSS6/3 surfactant solutions with concentration of 0.05−1 wt % were used for wetting experiments. The water−surfactant mixtures were

dx.doi.org/10.1021/la403994y | Langmuir 2013, 29, 14855−14864

hand shaken vigorously in order to disperse the surfactants. They were used within 24 h after preparation. Thus, the influence of hydrolytic degradation of such aqueous solutions could be neglected.

The static surface tension of all aqueous surfactant solutions are measured by the pendent drop technique with the Profile Analysis Tensiometer, and all results are summarized in Table 1. For aqueous ionic surfactants solutions, the surface tension is 55 mN/m with concentration 0.1 CMC, and it decreases to 32 mN/m at/above the CMC. All used trisiloxane solutions have concentrations well above CMC, which is supposed to be approximately 0.005 wt %. The surface tensions of trisiloxane solutions above CMC were more or less identical (22 mN/m) in the entire range of concentrations studied (0.05−1 wt %). The study of trisiloxane solutions below CMC is beyond the work, because such solutions will not show superspreading.

Table 1. Values of Surface Tension (at T = 22 °C) and Molecular Weight of Aqueous Surfactant Solutions[a]

surfactant	molecular formula	concentration	γ (mN/m)	molecular weight (g/mol)
CTAB	$CH_3(CH_2)_{15}N(CH_3)_3Br$	0.1 CMC	55	364
		1−3 CMC	32	
SDS	$CH_3(CH_2)_{11}OSO_3Na$	0.1 CMC	55	288
		1−3 CMC	32	
TSS10/2	M(D'EO_{10} PO_2 OH)M	0.05−1 wt %	22	850
TSS6/3	M(D'EO_6 PO_3 OH)M	0.05−1 wt %	22	700

[a]The standard deviation in the surface tension measurement was ∼1 mN/m.

3.2. Dynamic Wetting Experiments. The PP film was adhered to a glass slide by sandwiching a thin layer of ethanol between them. After ethanol evaporated, the PP film was flatly fixed on the glass slide. Then the PP substrate was put on a vertical stage controlled by a micrometer screw in a closed chamber, through which experiment temperature and relative humidity were controlled. A steel needle with an outer diameter of 400 μm was placed above the substrate at a certain distance for drop generation. The needle was prior hydrophobized with 1,1,1,3,3,3-hexamethyldisilazane (Roth GmbH, Germany) in a desiccator at room temperature for 12 h. This prevented the drops wetting the needle. Aqueous surfactant drops with radii 0.7−1.5 mm were produced with a syringe pump and gently deposited onto the substrates by approaching the substrate driven by the micrometer screw. The approach speed of drops to the surface was a few micrometers per second, which was verified by high-speed video imaging. A cold light source with a diffuser, which allowed uniform lighting and good contrast, was used for illumination. The early spreading process ($t \leq 1$ s) was captured from side view with a high-speed video camera (FASTACAM SA-1, Photron Inc., U.S.A.) at a rate of 54,000 fps. The side view of spreading drops suffers from the limitation of spatial resolution in the case of superspreading, as a very thin liquid film will be formed with immeasurable contact angle (below 8°) and radius due to complete loss of the spherical shape of the drop and its subsequent distortion. Therefore, for the late wetting process (1 s < t < 9 s), the top view was monitored with another high speed camera (Mikrotron GmBH, Germany) at a rate of 150 fps. All experiments were conducted at room temperature (22 ± 1 °C) and relative humidity of 40 ± 5%. During the spreading experiments, the change of the drop mass due to evaporation was less than 5%. So, evaporation effects could be neglected. To ensure reproducibility, spreading experiments were repeated at least four times with each liquid on fresh PP substrates.

3.3. Data Analysis. *Image Processing.* Recorded image sequences of the spreading drops were analyzed with a self-programmed MATLAB (MathWorks Inc., U.S.A.) algorithm and C++ (Visual Studio 6.0) algorithm. We identified the contact contour between the drop and substrate by subtracting the image background of the first figure. Supposing that the spreading drops in the early stage take a spherical shape, the contact angle of spreading drops can be determined from contact radius directly. From each image we extracted the contact radius and/or the contact angle from the drop profiles.

Data Fitting. We analyzed the wetting data in the second stage with G-dyna software, which was described in detail by Seveno et al.[44] To determine the wetting velocity at the TPCL, the dependence on time of drop radius is fitted by a polynomial function. This function is such that it has a maximum order of 10. However, we were able to accurately fit our contact radius versus time curves in our range of interest with polynomials of order 2. The velocity of the contact-line versus time was calculated by differentiating the obtained functions numerically. Both HD and MKT models, embedded in the G-dyna software, were chosen for data fitting.

4. RESULTS AND DISCUSSION

4.1. Dynamic Wetting of Aqueous Surfactant Solutions of CTAB and SDS. The dynamic wetting of pure water and aqueous surfactant solutions of CTAB and SDS with different concentrations (0.1−3 CMC) on PP substrates was studied. All drops spread out spontaneously after contacting the PP substrates. Figure 1 shows the spreading radius r as a function of the spreading time t of aqueous conventional surfactants. When a small amount of surfactant is added to water, the drops initially spread with an average velocity $V \sim$ 0.15m/s, which is slightly faster than that of pure water (∼ 0.1 m/s). It is well-known that the early wetting dynamics of pure liquids is dominated by inertia and the spreading radius grows according to a power law.[26−28] The log−log plots in Figure 1a,b indicate that in the presence of surfactants, the spreading radius

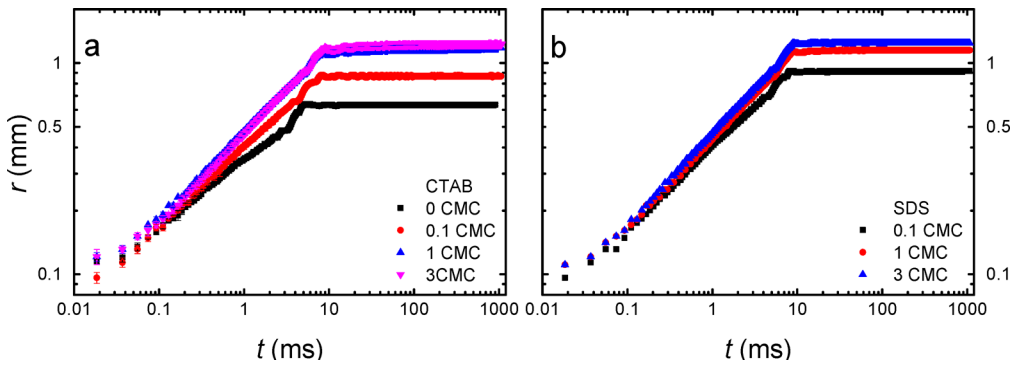

Figure 1. (a,b) Spreading radius versus time of pure water and aqueous surfactant solutions of CTAB and SDS on PP substrates in a log−log representation (0 CMC denotes pure water). The data was averaged from several repeated experiments. The error bars show that the experiments were very reproducible. For clarity, the error bars were omitted in other figures.

dx.doi.org/10.1021/la403994y | Langmuir 2013, 29, 14855−14864

follows a power law as well. For all liquids, only one inertia-dominated spreading stage was found. This fast spreading process lasted approximately 10 ms. After that, the conventional surfactant solutions did not spread further on PP substrates, as we expected. Our observations were in good agreement with previous reports,[45,46] where the authors showed conventional ionic surfactants did not promote rapid spreading of water drops on substrates as hydrophobic as PP films.

As mentioned in Section 2, on rigid substrates the actual duration τ of the early inertial stage of pure liquids shows a linear dependence on the characteristic inertial time τ_c. With surfactant addition, we experimentally found that τ was also linearly dependent on τ_c, as shown in Figure 2. A linear fitting

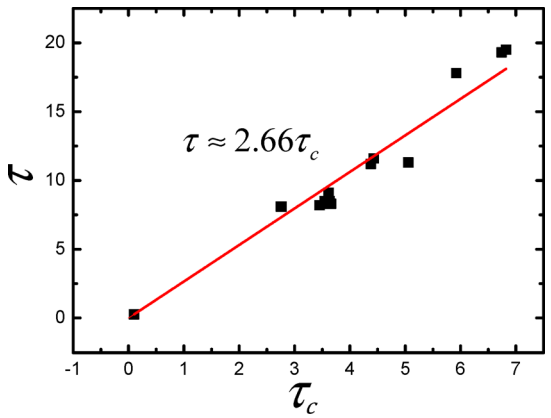

Figure 2. Inertial wetting time of drops of various liquids and sizes on PP substrates as a function of characteristic inertial time τ_c. The solid line is the best fit with slope 2.66.

gives a slope of ~2.66, which is very close to the value of ~2.82 reported in ref 27. This indicates that the addition of surfactant has no effect on the duration of the inertial wetting stage.

Figure 3 summarizes the wetting exponents α and the static contact angles θ_0 for pure water, CTAB, and SDS during the early spreading stage. The exponent is ~0.33 for pure water, which is consistent with values on hydrophobic substrates in previous studies.[27,28] The exponents of aqueous surfactant solutions are larger than that of water, and they increase with increasing surfactant concentration. This is due to the decrease of surface tension with surfactant addition (Table 1). However, for aqueous solutions above CMC, the spreading dynamics varies little and the spreading exponents remain unchanged. As shown in Figure 3a, the static contact angle θ_0 decreases with increasing surfactant concentration and decreasing surface tension. Also, the exponent depends on the static contact angle θ_0 (Figure 3b). Our observations are in good agreement with findings that the inertial spreading exponent is only dependent on substrate wettability or liquid surface tension.[27,28]

4.2. Aqueous Trisiloxane Surfactant Solutions. *Fast (or Inertial) Wetting Stage.* In this part, we investigated the wetting dynamics of two trisiloxane surfactant solutions (TSS10/2 and TSS6/3) with concentrations from 0.05 to 1 wt %. The log−log plots of spreading radius $r(t)$ versus time of the trisiloxane drops in the time window 0−1 s are shown in Figure 4. For CTAB and SDS solutions, we only observed inertial spreading before the drops stopped spreading. In contrast, the spreading process of both aqueous trisiloxane surfactant solutions could be subdivided into two stages: a fast spreading followed by a slower spreading stage setting in after ~12 ms. The fast spreading stage, with an average velocity of ~0.15 m/s, was also dominated by inertia and followed a power law with exponent $\alpha \sim 0.42$ (Figure 4). Lee et al.[18] observed that the first fast stage was characterized by power laws with exponents between 0.4 and 0.8, depending on the surfactant types and solubility. However, the short time regime in their study is $10 \lesssim t \lesssim 100$ ms, which is not comparable to the time scale in our work ($t \lesssim 12$ ms). The close similarity in the spreading of r versus t for early times was observed over the entire concentration range studied (0.05−1 wt %). Moreover, the duration of the initial stage τ was linearly dependent on the characteristic inertial time τ_c, which was observed also for water, CTAB, and SDS (Figure 2). Therefore, we conclude that the surfactant types and concentrations do not influence the duration of the initial inertia-dominated spreading regime in the concentration range we used.

Slow (or Viscous) Wetting Stage. For aqueous TSS10/2 solutions (Figure 4a), the spreading process slowed down after the fast inertial stage and the spreading dynamics was more or less similar for different concentrations except low concentration 0.05 wt %. Compared with TSS10/2, the spreading of TSS6/3 drops was slightly faster for $t \gtrsim 12$ ms, and the effects of concentration became gradually more evident (Figure 4b). After 1 s, the drops of TSS6/3 solutions became flat micrometer-thick puddles with contact angles below ~8°.

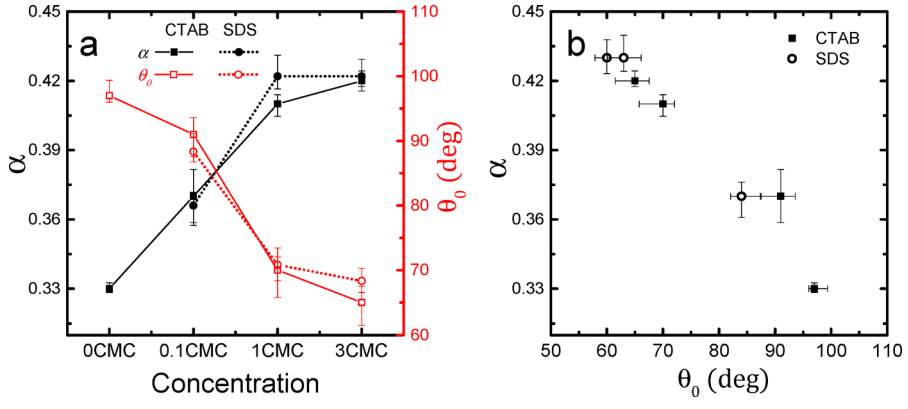

Figure 3. (a) Exponent α and static contact angle θ_0 plotted as a function of surfactant concentration. (b) Exponent α versus static contact angle θ_0 for water, CTAB and SDS (0.1−3 CMC).

dx.doi.org/10.1021/la403994y | *Langmuir* 2013, 29, 14855−14864

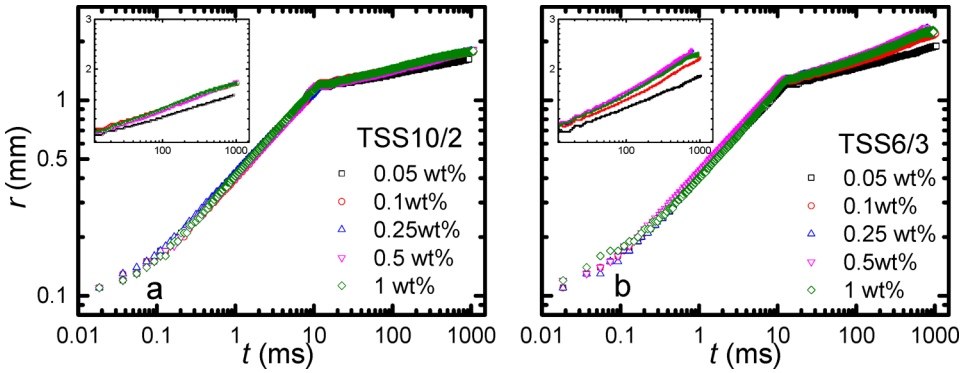

Figure 4. Log–log plots of spreading radius r versus time t of aqueous TSS10/2-laden drops (a), and aqueous TSS6/3-laden drops (b). Insets zoom in the spreading curves in the second stage of wetting.

Thus, we had no access to the drop profiles from the side due to the resolution limits of the optical technique. Nevertheless, we managed to capture the spreading process for a longer period of time from top view, which will be discussed later.

The second spreading stage ($t \gtrsim 12$ ms) could also be fitted with a power law using a standard least-squares method. Figure 5 shows the exponents of aqueous TSS10/2 and TSS6/3

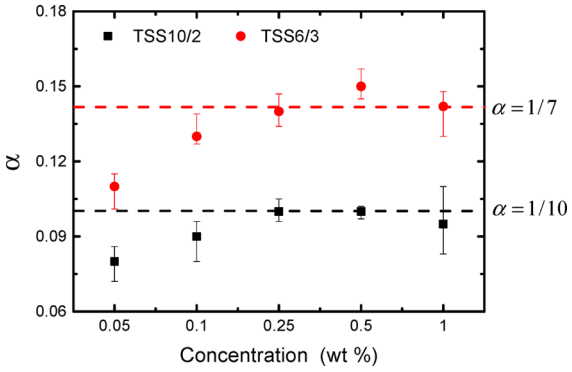

Figure 5. Exponent α for trisiloxane surfactant solutions at different concentrations.

surfactant solutions with different concentrations. For TSS10/2 solutions, the drop radius showed a time-dependence of $r \propto t^{1/10}$. In contrast, aqueous TSS6/3 solutions had a higher scaling coefficient of $r \propto t^{1/7}$. Despite the use of different substrates, the exponents are quite close to those reported in ref 18 where the authors also fitted the spreading dynamics at $100 \lesssim t \lesssim 1000$ ms with a power law. Considering the dynamic wetting models outlined in Section 2, it could appear that the wetting dynamics of TSS10/2 solutions is better described by the HD model, while the MKT model better describes the wetting dynamics of TSS6/3 solutions. To verify this, both HD and MKT models were used to fit experimental data of TSS10/2 and TSS6/3 surfactant solutions (Figure 6). As inertial spreading is not included in the models, it was also not used to fit data in the inertial regime. Therefore, we masked this data between 0 and 12 ms and analyzed the second (slower) spreading stage only.

Figure 6 shows the dynamic contact angles θ versus spreading velocity V for drops of TSS10/2 and TSS6/3 solutions with concentration 0.1 wt % on PP substrates. After the inertial stage, the spreading of both drops continued with a contact angle of ~68° and a velocity of ~0.001 m/s (top right corner of the graph), and then proceeded toward smaller

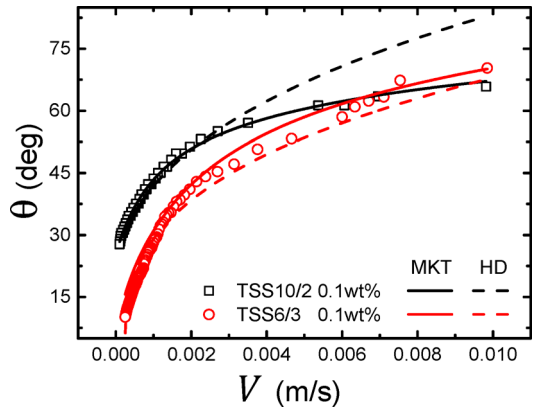

Figure 6. Dynamic contact angle versus spreading velocity for the drops of two trisiloxane surfactant solutions at 0.1 wt %. The best fit of MKT and HD models were represented by different lines. Fit parameters were listed in Table 2.

contact angles and lower velocities. For aqueous solutions with low-surfactant concentrations as studied by us, the density and viscosity did not differ much from that of pure water. Therefore, the values used in the fitting process were those of pure water and the corresponding HD and MKT parameters are listed in Table 2.

Table 2. Parameters ln L/L_s, K_0 (MHz), λ (nm), and θ_0(deg) Fitted by HD, MKT, and θ^{exp} from Experimental Results

	ln L/L_s	θ_0^{HD}	K_0	λ	θ_0^{MKT}	θ^{exp}
TSS10/2 @ 0.1 wt %	820	26	0.24	1.55	26	25
TSS6/3 @ 0.1 wt %	469	~0	0.8E6	1.16	~0	8

As shown in Figure 6, the MKT model provides a very good fit to the experimental results over the whole data set of TSS10/2 0.1 wt %, while the HD model is only accurate for the low velocity regime. The obtained values of the parameters from the MKT fit are reasonable, and the fitted values of θ_0^{MKT} deviate little from the experimental value (see Table 2). The derived value of In L/L_s from the HD fit leads to a subatomic slip length, which has therefore limited physical meaning.[47,48] In comparison, the fits to the wetting dynamics of TSS6/3 with the MKT and HD models are poor, and the obtained parameter values, K_0 (typically 1 MHz) and ln L/L_s (typically 10), are physically unsound. Despite these parameters, the HD fit seems to fairly agree with the experiment results of TSS10/2 and TSS6/3 solutions at low velocity (small values of contact

dx.doi.org/10.1021/la403994y | Langmuir 2013, 29, 14855–14864

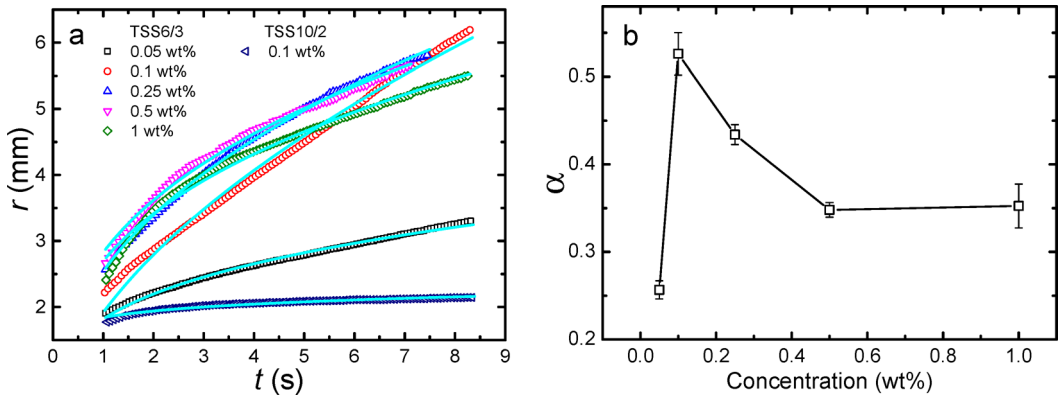

Figure 7. (a) Drop spreading radius versus time of aqueous trisiloxane surfactant solutions at various concentrations on PP substrates in the late spreading stage. Solid lines represented the power law fits to experiment results. The exponent α for aqueous TSS6/3 solutions at different concentrations was plotted in (b).

angle). Similar observation could be found in ref 49, the findings in which showed the HD model was valid for small angles (low-velocity data) in the presence of a surfactant. Moreover, the hydrodynamic regime was preceded by a molecular-kinetic regime at high velocity.[49] Such conclusion fails to work for TSS6/3 solution here; since the MKT fit to the TSS6/3 solution is poor at high velocity (Figure 6). Nevertheless, Hopf et al.[50] reported that for surfactant-containing system, the HD model was in accord with the experimental results for a high three-phase-contact velocity, while MKT model held only for a small velocity. The authors in ref 51 also observed a deviation from the theoretical trend given by MKT model at high velocities. These discrepancies may result from different surfactant properties which will influence the surfactant transfer to the liquid/vapor and to solid/vapor interface, thus affecting the dynamic contact angles during advancing three phase contact motion.

The experimental spreading data of trisiloxane solutions at other concentrations were also fitted with HD and MKT models (see fitting parameters in Supporting Information). Overall, the two models prove to be inappropriate to describe the wetting of TSS6/3 solutions. Reasonable agreement is obtained with MKT and TSS10/2 solutions, and poor agreement is obtained with the HD model and TSS10/2 solutions. This result was somehow disappointing based on the previous observation that the experimental wetting exponents corresponded to those predicted by the HD (for TSS10/2) and MKT (for TSS6/3) models for fully wetting liquids. This leads us to conclude here that both dynamic wetting models, originally developed for pure liquids, cannot be generally applied to (our) experiments with surfactant solutions. In fact, because of the presence of surfactants in the drops, surface tension gradients or dynamic surface tension effects result from different molecular mobility and interfacial adsorption, while the HD and the MKT models do not take into account dynamic interfacial tensions that are more pronounced at larger wetting velocities. However, the suitability of the MKT model for the description of the spreading of TSS10/2 solutions, but not of the TSS6/3 solutions, might imply that the effect of dynamic surface tension is even more important for the superspreading behavior, and that the dynamics of surfactant molecules at the TPCL is generally different for the two trisiloxane surfactants. This was also suggested[2,9,10,21,23] where the authors proposed that the nonsuperspreading surfactant formed micellar aggregates, while the superspreading surfactant formed easily "unzippable" bilayer microstructures at the leading edge, especially in the case of an L_3 or L_α phase. This idea was also supported by experimental observations in other studies:[52,53] nonsuperspreaders with longer hydrophilic groups form micellar solutions, rather than a L_3 or L_α phase formed by superspreaders. The bilayer configuration of the TSS6/3 trisiloxane molecules would enable their direct and rapid transfer to the air/water interface and to the solid substrate at the TPCL. As pointed out by Kumar et al.,[23] direct adsorption of bilayer aggregates to the air/water interface is one possibility to augment the surfactant adsorptive flux and maintain a high concentration at the drop apex. The question remains about the driving force that causes advection of the more easily unzipping bilayers to the contact line region.

Superspreading Stage. As shown in Figure 4b, the spreading of aqueous TSS6/3 solutions at different concentrations accelerated after ~100 ms, which implied that the spreading in the second regime was not just controlled by the viscosity and the surface tension of the liquid, but driven by one or more additional effects. We recorded the spreading radius of drops for $t > 1$ s from a top view (Figure 7a). For comparison with the superspreading TSS6/3 solutions, the spreading dynamics of TSS10/2 0.1 wt % is also shown. Drops with TSS10/2 stopped spreading with a measurable static contact angle of ~12° on the PP substrates. Contrarily, drops with TSS6/3 at all concentrations completely wetted the PP substrates in the end, with a hardly measurable macroscopic contact angle close to 0°. Not only the final contact angles, but the spreading dynamics between 1 and 10 s of TSS10/2 and TSS6/3 solutions at several concentrations were remarkably different as well. One reason might lie in the different length of hydrophilic EO chain of TSS10/2 and TSS6/3. Ruckenstein[22] theoretically argued that only surfactants with moderately long hydrophilic chains (7−8 EO groups) are able to induce strong spreading of water on hydrophobic substrates, whereas longer hydrophilic chains prefer to interact with water and decrease the adsorbability of the surfactant to the interfaces, thus reducing the spreading efficiency. The argument that surfactants with intermediate EO chain length show unusually fast spreading on hydrophobic substrates has been experimentally verified.[21,54] It was also reported that surfactants forming turbid dispersions in water performed better than those forming clear micellar solutions.[2,8] A visual inspection of TSS6/3 and TSS10/2 solutions showed that the TSS6/3 solutions were slightly milky or turbid above a concentration of

dx.doi.org/10.1021/la403994y | *Langmuir* 2013, 29, 14855−14864

~0.1 wt %. TSS10/2 solutions were clear even at a concentration of ~0.5 wt %, owing to their increased solubility due to their longer hydrophilic tails. Dynamic light scattering (DLS) measurements (data not shown here) revealed aggregates with sizes ranging from 30 to 800 nm in the TSS6/3 solutions, while the aggregates in the TSS10/2 solutions had sizes of ~10 nm and were nearly monodispersed. The nonuniform aggregates in TSS6/3 may be associated with the known bilayered L_3 or L_α structures of superspreaders, while the uniform micellar structures in TSS10/2 are similar to those known for most conventional surfactants.[9]

In the present work we did not determine the final wetted area of aqueous superspreader solutions with different concentrations because of the limits of our optical imaging technique. When superspreading occurred, the final drop profile was so thin that we could not distinguish it from the transparent PP substrate and the contour of the wetted area was not circular any more, but started to show pronounced fingering. We stopped investigations before 10 s, when all drops still showed circular contours. However, as shown in Figure 7a, drop radii within 9 s differed much for all solutions investigated. Different concentrations of TSS6/3 solutions significantly influenced the spreading dynamics and the wetted area. Solutions with concentration of 0.05 wt % spread slowest and wetted the least, while solutions with higher concentrations spread faster to larger wetted area. At the beginning (<3 s), the spreading velocity and wetted area increased with concentration, but kept more or less identical above a certain concentration (0.1 wt %). Deceleration of the spreading process was observed after 3 s for solutions with concentration >0.1 wt %. Considering the entire spreading process, the average spreading velocity and wetted area were maximum at the concentration of 0.1 wt %. Similar results were reported in literature,[2,14,55,56] although the employed trisiloxane surfactants and hydrophobic substrates were different from the ones in our study. The spreading velocity during the first 10 s of the spreading process was investigated as a function of concentration in ref 55, where it was found that at low concentrations, the spreading velocity was proportional to surfactant concentration, but above a certain limit (0.1 wt %) the velocity became constant.

The spreading radius in the superspreading regime could also be fitted with a power law. Although some curves could not be perfectly fitted over the whole time range from 1 to 9 s, fitting was still acceptable with a correlation coefficient above 0.98. The exponent of the power law for TSS6/3 solutions spreading at all concentrations ranged from one-fourth to one-half (Figure 7b). These results were in fair agreement with previous work.[14,16,57,58] The slow spreading dynamics of pure liquids on completely wetting substrates is well described by Tanner's law $r \propto t^{1/10}$.[32] Thus, TSS6/3 solutions showed a much faster spreading than pure liquids; hence, the HD and MKT models do not allow drawing conclusions on the wetting mechanisms active here. Since Marangoni forces can lead to $r \propto t^{1/4}$,[59,60] they have been considered to be a reasonable explanation for the fastening of the spreading of aqueous surfactant solutions after a spreading time of ~1 s.[8,12,14,16,23]

The influence of surfactant concentration on Marangoni effects could be explained in this way. At low concentration (0.05 wt %), the rate of surfactant diffusion from the bulk to the newly created fresh drop surface is slow, as the surfactant concentration gradient is small. Eventually, a radial surface tension gradient can be formed and lead to a power law spreading dynamics of $r \propto t^{1/4}$. By increasing the surfactant concentration to 0.1 wt %, the larger surface tension gradient provides a stronger driving force, and as a consequence a higher velocity and a larger extent of spreading. A further increase of surfactant concentration leads to a larger spreading velocity at the beginning due to a stronger driving force. However, the spreading in the late stage slows down, because the surfactant diffusion from the bulk is fast enough to replenish surfactant in the newly created drop surface. Therefore, the interface is saturated with surfactants rapidly, and the surface tension gradient fades more quickly. As a result, a critical concentration (0.1 wt %) does exist for our system at which the spreading velocity and the area wetted by a drop are maximum due to a balance between surface tension gradient driving the drop spreading and the rate of surfactant diffusion to the water−air interface reducing the surface tension gradient. The different exponents of surfactant solutions with different concentrations, laying between one-fourth and one-half, imply that the surface tension gradient is probably established in the radial and in the normal direction, as suggested also in ref 16. Spreading dynamics is set by a dynamic surface tension gradient, which depends on the competing process of the growth rate of fresh water−air interface and the diffusion rate of surfactant from bulk to the water−air interface.[23] The rate of adsorption of the surfactants at such interface is not high enough to maintain the apex tension low. However, it is possible that direct adsorption of bilayer aggregates of superspreader enhances the monomer flux, which alone is insufficient to maintain an effective Marangoni gradient. These arguments offer a reasonable interpretation of the results shown in Figure 7a. Drops of TSS10/2 solutions with micelles fail to superspread. A surface tension gradient sufficient to sustain the wetting process of drops is maintained for the longest time for aqueous TSS6/3 solutions with a characteristic concentration of 0.1 wt %. For these reasons, these drops continue spreading rapidly and constantly, and cross the spreading curves of the drops with higher concentrations at some time (Figure 7a). The reasons why exactly solutions with concentration 0.1 wt % show the best wetting performance under these experimental conditions (drop size, surface wettability, and relative humidity) are still unclear and beyond the scope of this work. Although the above considerations offer a simplified picture, they suggest that the Marangoni force is a major driving force in the superspreading regime.

5. SUMMARY

We carried out a systematic study on the wetting dynamics of aqueous solutions of conventional ionic surfactants (CTAB, SDS) and nonionic trisiloxane surfactants (TSS10/2, TSS6/3) with different concentrations on hydrophobic polypropylene substrates. In all experiments, the circular spreading radius of the drops was monitored with a high speed camera. We could show that depending on the surfactants one, two, or three stages of dynamic wetting occurred, and that each stage could be roughly characterized by power law dynamics. The advancement of all aqueous drop rims first followed a power law with exponent between 0.3 and 0.45 in a short-time window (<12 ms). Thus early wetting dynamics was mainly controlled by capillary forces and inertia, and the type of surfactant and its concentration did not play a role. Alternatively, for CTAB and SDS solutions only this wetting stage was observed before the drops stopped spreading and attained a well-defined contact angle and contact radius. Both

trisiloxane solutions showed an additional and similar slower wetting regime after the inertial stage. TSS6/3 solutions at any concentration spread only slightly faster than TSS10/2 solutions during this stage that lasted from ∼12 ms to ∼1 s. This stage corresponded to the one usually dominated by capillarity and viscous forces, and the exponents of the power laws describing the wetting were between 0.1 (TSS10/2) and 0.15 (TSS6/3). At the end of this stage, the TSS10/2 drops approached equilibrium with well-defined contact angle and contact radius and reached it for times <5 s. Only the TSS6/3 drops showed a third, so-called superspreading regime. During this stage, drop spreading on PP was strongly dependent on surfactant concentration. Strikingly, the spreading velocity increased again and the maximum average velocity was observed at a concentration of 0.1 wt %. The power law exponents derived from fits to the experimental data varied with concentration and ranged from 0.25 to 0.55, that is, they were larger than the exponents during the second spreading stage. We argue that the additional driving force accelerating wetting during the superspreading stage is due to Marangoni effects caused by surface tension gradients, which developed in a time between 0.1 and 1 s, and were fully effective thereafter. On the plausible reasons why the spreading efficiency is dependent on concentration, we can only speculate that an effective surface tension gradient results from an optimum balance between the rate of drop expansion and the rate of surfactant diffusion from the bulk to the water−air interface, and a critical surfactant concentration is required to maintain a sufficient surface tension gradient over a long time. For higher concentrations, the surface tension gradient decreases quickly during spreading due to a faster diffusion of surfactant to the drop interface. It is known that evaporation and relative humidity also affect the final wetted area of superspreading solutions, since upon evaporation the concentration of surfactant increases at the rim of the drops and the spreading efficiency decreases.[9,55] However, due to the short observation time window in our work we did not find evidence that the evaporation of water at RH = 40% did influence the results considerably. The influence of relative humidity on the late spreading dynamics will be studied systematically in future work.

■ ASSOCIATED CONTENT

Supporting Information

Table with an extended list of the fitting parameters ln L/L_s, K_0 (MHz), λ (nm), and θ_0(deg) from HD and MKT fits, and θ^{exp}(deg) from experiments. This material is available free of charge via the Internet at http://pubs.acs.org.

■ AUTHOR INFORMATION

Corresponding Author

*E-mail: bonaccurso@csi.tu-darmstadt.de.

Notes

The authors declare no competing financial interest.

■ ACKNOWLEDGMENTS

We acknowledge beneficial discussions with Marcus Lopes and Lars Heim. This research was supported by the German Research Foundation (DFG) within the Cluster of Excellence 259 “Smart Interfaces − Understanding and Designing Fluid Boundaries”.

■ REFERENCES

(1) Ananthapadmanabhan, K. P.; Goddard, E. D.; Chandar, P. A study of the solution, interfacial and wetting properties of silicone surfactants. *Colloids Surf.* **1990**, *44*, 282−97.

(2) Hill, R. M. Superspreading. *Curr. Opin. Colloid Interface Sci.* **1998**, *3*, 247−254.

(3) Karsa, D. R. *Industrial Applications of Surfactants*; Royal Society of Chemistry: Cambridge, U.K., 1987.

(4) Knoche, M. Organosilicone Surfactant Performance in Agricultural Spray Application - A Review. *Weed Res.* **1994**, *34* (3), 221−239.

(5) Schwartz, E.; Reid, W. *Ind. Eng. Chem.* **1994**, *56*, 26.

(6) Kanner, B.; Reid, W. G.; Petersen, I. H. Synthesis and Properties of Siloxane-Polyether Copolymer Surfactants. *Ind. Eng. Chem. Res.* **1967**, *6* (2), 88−92.

(7) Murphy, G. J.; Policello, G. A.; Ruckle, R. E. Formulation Considerations for Trisiloxane Based Organosilicone Adjuvants. *Brit Crop. Prot. Conf.* **1991**, 355−362.

(8) Zhu, S.; Miller, W. G.; Scriven, L. E.; Davis, H. T. Superspreading of water-silicone surfactant on hydrophobic surfaces. *Colloids Surf., A* **1994**, *90*, 63−78.

(9) Venzmer, J. Superspreading — 20 years of physicochemical research. *Curr. Opin. Colloid Interface Sci.* **2011**, *16* (4), 335−343.

(10) Maldarelli, C. On the microhydrodynamics of superspreading. *J. Fluid Mech.* **2011**, *670*, 1−4.

(11) Hill, R. M.; He, M. T.; Davis, H. T.; Scriven, L. E. Comparison of the Liquid-Crystal Phase-Behavior of 4 Trisiloxane Superwetter Surfactants. *Langmuir* **1994**, *10* (6), 1724−1734.

(12) Chengara, A.; Nikolov, A. D.; Wasan, D. T. Spreading of a water drop triggered by the surface tension gradient created by the localized addition of a surfactant. *Ind. Eng. Chem. Res.* **2007**, *46* (10), 2987−2995.

(13) Nikolov, A.; Wasan, D. Superspreading: Role of the Substrate Surface Energy. In *Without Bounds: A Scientific Canvas of Nonlinearity and Complex Dynamics, Understanding Complex Systems*; Rubio, R. G., Ryazantsev, Y. S., Starov, V. M., Huang, G.-H., Chetverikov, A. P., Arena, P., Nepomnyashchy, A. A., Ferrus, A., Morozov, E. G., Eds.; Springer Verlag: Berlin, 2013.

(14) Nikolov, A. D.; Wasan, D. T.; Chengara, A.; Koczo, K.; Policello, G. A.; Kolossvary, I. Superspreading driven by Marangoni flow. *Adv. Colloid Interface Sci.* **2002**, *96* (1−3), 325−338.

(15) Ivanova, N.; Starov, V.; Johnson, D.; Hilal, N.; Rubio, R. Spreading of Aqueous Solutions of Trisiloxanes and Conventional Surfactants over PTFE AF Coated Silicone Wafers. *Langmuir* **2009**, *25* (6), 3564−3570.

(16) Rafai, S.; Sarker, D.; Bergeron, V.; Meunier, J.; Bonn, D. Superspreading: Aqueous surfactant drops spreading on hydrophobic surfaces. *Langmuir* **2002**, *18* (26), 10486−10488.

(17) Rosen, M. J.; Song, L. D. Superspreading, Skein Wetting, and Dynamic Surface Tension. *Langmuir* **1996**, *12* (20), 4945−4949.

(18) Lee, K. S.; Starov, V. M.; Muchatuta, T. J. P.; Srikantha, S. I. R. Spreading of trisiloxanes over thin aqueous layers. *Colloid J.* **2009**, *71* (3), 365−369.

(19) Lee, K. S.; Starov, V. M. Spreading of surfactant solutions over thin aqueous layers: Influence of solubility and micelles disintegration. *J. Colloid Interface Sci.* **2007**, *314* (2), 631−642.

(20) Knoche, M.; Tamura, H.; Bukovac, M. J. Performance and Stability of the Organosilicone Surfactant L-77 - Effect of pH, Concentration, and Temperature. *J. Agr. Food Chem.* **1991**, *39* (1), 202−206.

(21) Stoebe, T.; Lin, Z. X.; Hill, R. M.; Ward, M. D.; Davis, H. T. Surfactant-enhanced spreading. *Langmuir* **1996**, *12* (2), 337−344.

(22) Ruckenstein, E. Effect of short-range interactions on spreading. *J. Colloid Interface Sci.* **1996**, *179* (1), 136−142.

(23) Kumar, N.; Couzis, A.; Maldarelli, C. Measurement of the kinetic rate constants for the adsorption of superspreading trisiloxanes to an air/aqueous interface and the relevance of these measurements to the mechanism of superspreading. *J. Colloid Interface Sci.* **2003**, *267* (2), 272−285.

(24) de Gennes, P. G. Wetting: statics and dynamics. *Rev. Mod.Phys.* **1985**, *57*, 827−863.
(25) de Gennes, P. G.; Brochard-Wyart, F.; Quere, D. *Capillarity and Wetting Phenomena*; Springer: New York, 2004.
(26) Biance, A. L.; Clanet, C.; Quere, D. First steps in the spreading of a liquid droplet. *Phys. Rev. E* **2004**, *69* (1), 016301.
(27) Chen, L.; Auernhammer, G. K.; Bonaccurso, E. Short time wetting dynamics on soft surfaces. *Soft Matter* **2011**, *7* (19), 9084−9089.
(28) Bird, J. C.; Mandre, S.; Stone, H. A. Short-time dynamics of partial wetting. *Phys. Rev. Lett.* **2008**, *100*, (23).
(29) Chen, L.; Bonaccurso, E.; Shanahan, M. E. R. Inertial to Viscoelastic Transition in Early Drop Spreading on Soft Surfaces. *Langmuir* **2013**, *29* (6), 1893−1898.
(30) Lamb, H. *Hydrodynamics*; Dover: New York, 1932.
(31) de Gennes, P. G. *C. R. Acad. Sci., Ser. II* **1984**, *298*, 111−115.
(32) Tanner, L. The spreading of silicone oil drops on horizontal surfaces. *J. Phys. D: Appl. Phys.* **1979**, *12*, 1473.
(33) Cazabat, A. M.; Cohen-Stuart, M. A. Dynamics of Wettlng: Effects of Surface Roughness. *J. Phys. Chem.* **1986**, *90*, 5845−5849.
(34) Blake, T. D.; Haynes, J. M. Kinetics of Liquid/Liquid Displacement. *J. Colloid Interface Sci.* **1969**, *30* (3), 421−&.
(35) Blake, T. D.; Ruschak, K. J. Maximum Speed of Wetting. *Nature* **1979**, *282* (5738), 489−491.
(36) Cox, R. G. The dynamics of the spreading of liquids on a solid surface. Part 2. Surfactants. *J. Fluid Mech.* **1986**, *168*, 195−220.
(37) Voinov, O. V. Hydrodynamics of wetting. *Fluid Dyn.* **1976**, *11*, 714−721.
(38) Cazabat, A. M. Wetting - from Macroscopic to Microscopic Scale. *Adv. Colloid Interface Sci.* **1992**, *42*, 65−87.
(39) Hoffman, R. L. Study of Advancing Interface 0.1. Interface Shape in Liquid-Gas Systems. *J. Colloid Interface Sci.* **1975**, *50* (2), 228−241.
(40) Fermigier, M.; Jenffer, P. An Experimental Investigation of the Dynamic Contact-Angle in Liquid Liquid-Systems. *J. Colloid Interface Sci.* **1991**, *146* (1), 226−241.
(41) Cazabat, A. M.; Gerdes, S.; Valignat, M. P.; Villette, S. Dynamics of wetting: From theory to experiment. *Interface Sci.* **1997**, *5* (2−3), 129−139.
(42) de Ruijter, M. J.; De Coninck, J.; Blake, T. D.; Clarke, A.; Rankin, A. Contact Angle Relaxation during the Spreading of Partially Wetting Drops. *Langmuir* **1997**, *13* (26), 7293−7298.
(43) Fell, D.; Sokuler, M.; Lembach, A.; Eibach, T.; Liu, C.; Bonaccurso, E.; Auernhammer, G.; Butt, H.-J. Drop impact on surfactant films and solutions. *Colloid Polym. Sci.* **2013**, *291* (8), 1963−1976.
(44) Seveno, D.; Vaillant, A.; Rioboo, R.; Adao, H.; Conti, J.; De Coninck, J. Dynamics of Wetting Revisited. *Langmuir* **2009**, *25* (22), 13034−13044.
(45) Stoebe, T.; Hill, R. M.; Ward, M. D.; Davis, H. T. Enhanced Spreading of Aqueous Films Containing Ionic Surfactants on Solid Substrates. *Langmuir* **1997**, *13*, 7276−7281.
(46) Dutschk, V.; Sabbatovskiy, K. G.; Stolz, M.; Grundke, K.; Rudoy, V. M. Unusual wetting dynamics of aqueous surfactant solutions on polymer surfaces. *J. Colloid Interface Sci.* **2003**, *267* (2), 456−462.
(47) Fetzer, R.; Ramiasa, M.; Ralston, J. Dynamics of Liquid−Liquid Displacement. *Langmuir* **2009**, *25* (14), 8069−8074.
(48) Petrov, P. G.; Petrov, J. G. A Combined Molecular-Hydrodynamic Approach to Wetting Kinetics. *Langmuir* **1992**, *8* (7), 1762−1767.
(49) Roques-Carmes, T.; Mathieu, V.; Gigante, A. Experimental contribution to the understanding of the dynamics of spreading of Newtonian fluids: Effect of volume, viscosity, and surfactant. *J. Colloid Interface Sci.* **2010**, *344* (1), 180−197.
(50) Hopf, W.; Stechemesser, H. 3-Phase Contact Line Movement in Systems with and without Surfactant. *Colloids Surf.* **1988**, *33* (1−2), 25−33.
(51) Petrov, J. G.; Radoev, B. P. Steady Motion of the 3 Phase Contact Line in Model Langmuir-Blodgett Systems. *Colloid Polym. Sci.* **1981**, *259* (7), 753−760.
(52) Hill, R. M.; He, M.; Davis, T.; Scriven, L. Comparison of the Liquid Crystal Phase Behavior of Four Superwetter Surfactants. *Langmuir* **1994**, *10*, 1724−1734.
(53) Stoebe, T.; Lin, Z. X.; Hill, R. M.; Ward, M. D.; Davis, H. T. Enhanced Spreading of Aqueous Films Containing Ethoxylated Alcohol Surfactants on Solid Substrates. *Langmuir* **1997**, *13* (26), 7270−7275.
(54) Svitova, T.; Hoffmann, H.; Hill, R. M. Trisiloxane Surfactants: Surface Interfacial Tension Dynamics and Spreading on Hydrophobic Surfaces. *Langmuir* **1996**, *12* (7), 1712−1721.
(55) Venzmer, J.; Wilkowski, S. P. Trisiloxane Surfactants Mechanisms of Spreading and Wetting. In *Pesticide Formulations and Application System*; Nalewaja, J. D., Goss, G. R., Tann, R. S., Eds.; American Society for Testing and Materials - ASTM STP 1347: West Conshohocken, PA, **1998**; Vol. *18*.
(56) Lin, Z. X.; Hill, R. M.; Davis, H. T.; Ward, M. D. Determination of Wetting Velocities of Surfactant Superspreaders with the Quartz-Crystal Microbalance. *Langmuir* **1994**, *10* (11), 4060−4068.
(57) Chengara, A.; Nikolov, A.; Wasan, D. Surface tension gradient driven spreading of trisiloxane surfactant solution on hydrophobic solid. *Colloids Surf., A* **2002**, *206* (1−3), 31−39.
(58) Svitova, T.; Hill, R. M.; Radke, C. J. Adsorption layer structures and spreading behavior of aqueous non-ionic surfactants on graphite. *Colloids Surf., A* **2001**, *183*, 607−620.
(59) Gaver, D. P.; Grotberg, J. B. The Dynamics of a Localized Surfactant on a Thin-Film. *J. Fluid Mech.* **1990**, *213*, 127−148.
(60) Jensen, O. E.; Grotberg, J. B. Insoluble Surfactant Spreading on a Thin Viscous Film - Shock Evolution and Film Rupture. *J. Fluid Mech.* **1992**, *240*, 259−288.